CHEMIJA
2026. Vol. 37. No. 1. P. 1–11

ISSN 0235-7216 eISSN 2424-4538
DOI: https://doi.org/10.6001/chemija.2026.37.1.1

A reagentless amperometric glucose biosensor based on 5-amino-1,10-phenanthroline, gold nanoparticles and glucose oxidase

Katažyna Blaževič,

Aistė Krikštaponytė,

Anton Popov,

Almira Ramanavičienė,

Asta Kaušaitė-Minkštimienė*

NanoTechnas – Center of Nanotechnology and Materials Science,
Faculty of Chemistry and Geosciences,
Vilnius University,
24 Naugarduko Street,
03225 Vilnius, Lithuania

Glucose monitoring is essential for the management of diabetes and for ensuring an accurate analysis in clinical and food-related applications. In this study, a reagentless amperometric glucose biosensor was developed based on the layer-by-layer adsorption of 5-amino-1,10-phenanthroline (AP), 13 nm diameter gold nanoparticles (AuNPs), and glucose oxidase (GOx) onto a graphite rod electrode, followed by chemical cross-linking of GOx with glutaraldehyde vapour. AP acted as a redox mediator, enabling an efficient electron transfer, while AuNPs facilitated signal amplification. The biosensor exhibited a wide linear range (0.30–10.0 mM), low limits of detection and quantification (LOD 0.05 mM, LOQ 0.17 mM), a high repeatability (RSD 3.19%) and an acceptable reproducibility (RSD 5.51%), along with an excellent selectivity toward glucose and a satisfactory storage stability (86% signal retention over 7 days), and anti-interference performance against uric and ascorbic acids. These features demonstrate the biosensor's suitability for routine and point-of-care glucose monitoring. Furthermore, the proposed platform is versatile and can be adapted for the detection of other clinically or environmentally relevant analytes, highlighting its potential for broader analytical applications.

Keywords: reagentless amperometric glucose biosensor, 1,10-phenanthroline-5,6-dione, gold nanoparticles, glucose oxidase

INTRODUCTION

Diabetes mellitus is a group of metabolic disorders characterised by chronically elevated blood glucose levels. It represents one of the leading causes of morbidity and mortality worldwide and constitutes a major public health challenge, particularly in developed countries [1, 2]. The increasing prevalence of diabetes is closely associated with rising rates of obesity and lifestyle-related factors [3]. Monitoring of blood glucose levels is therefore essential for effective disease management and for preventing the progression of diabetes-related complications.

Among various analytical approaches, biosensors are considered one of the most effective tools for routine glucose monitoring in blood and urine samples [4]. In particular, amperometric glucose biosensors are among the most widely used and commercially available analytical devices due to their simplicity, high sensitivity, and suitability for miniaturisation [5]. These biosensors are typically based on enzymatic reactions involving either glucose oxidase (GOx) or glucose dehydrogenase. GOx is the most commonly employed enzyme in glucose sensing applications because of its high specificity toward glucose, excellent operational stability, resistance to extreme pH values, ionic strength, and temperature variations, as well as its relatively simple purification procedure and low cost [6]. For these reasons, GOx-based biosensors dominate the field of glucose analysis [7].

* Corresponding author. Email: asta.kausaite@chf.vu.lt

Depending on the generation of the biosensor, the amperometric determination of glucose using GOx-based biosensors relies on one of the following mechanisms: (1) anodic oxidation of hydrogen peroxide produced during the GOx-catalysed oxidation of glucose in the presence of dissolved oxygen; (2) cathodic reduction of oxygen; or (3) anodic oxidation of a redox mediator at the surface of the working electrode of the biosensor. The third approach offers significant advantages, as the analytical signal becomes independent of the partial pressure of oxygen and can be recorded at lower working potentials, thereby minimising interference from electroactive species present in the sample [8]. The redox mediator may be dissolved in the sample solution or immobilised on the working electrode surface together with the enzyme, forming a reagentless biosensing system. Although the first approach is simpler, immobilisation of the mediator on the electrode surface is more advantageous, as all components required for biosensor operation are confined to the electrode interface [9]. Consequently, no additional mediator needs to be added to the analyte solution after each measurement. Reagentless glucose biosensors can be applied in a variety of fields, from glucose detection in food and beverages to *in vivo* biomedical applications [10].

Currently, significant research efforts are focused on the development of glucose biosensors that are rapid, sensitive, selective, reliable, portable and cost-effective. To achieve these goals, novel materials are continuously explored to improve the analytical performance of biosensors [4]. Due to their unique physicochemical properties, gold nanoparticles (AuNPs) have attracted a considerable attention in the biosensor design. The incorporation of AuNPs into biosensing platforms can significantly enhance electron transfer efficiency and electrical conductivity, leading to improved sensitivity, selectivity, and both operational and storage stability of the biosensor [11–13].

In this work, a reagentless amperometric glucose biosensor was developed by sequential modification of a graphite rod (GR) electrode with 5-amino-1,10-phenanthroline (AP), AuNPs and GOx. To achieve optimal biosensor performance, the preparation conditions of the working electrode were systematically optimised, including the amounts of AP, AuNPs and GOx, and the duration of GOx cross-linking using glutaraldehyde (GA). In addition, key operational parameters such as the applied potential and the pH of the electrolyte solution were optimised. Subsequently, the main analytical characteristics of the developed biosensor were evaluated, including the linear detection range, limits of detection (LOD) and quantification (LOQ), reproducibility, repeatability, and storage stability. Furthermore, the selectivity of the biosensor and the influence of potential interferring substances on the analytical signal were investigated.

MATERIALS AND METHODS

Materials and reagents

GOx (*Aspergillus niger*, 360 U/mg protein), D(+)-glucose monohydrate, D(+)-galactose, D(+)-xylose, D(+)-mannose, CH_3COOH, KH_2PO_4, tannic acid, KCl, $Na_2HPO_4 \times 12\ H_2O$, NaOH, $HAuCl_4 \times 3\ H_2O$, trisodium citrate $\times$ 2 H_2O, and HCl acid were obtained from Carl Roth GmbH (Karlsruhe, Germany). AP, $CH_3COONa \times 3\ H_2O$, 25% aqueous solution of GA, L-ascorbic acid, and uric acid were purchased from Sigma-Aldrich Chemie GmbH (Steinheim, Germany). Ethanol absolute, D(-)-fructose, and D(+)-saccharose were obtained from Merck KGaA (Darmstadt, Germany).

Preparation of solutions

An acetate–phosphate buffer (APB) consisting of 0.05 M CH_3COONa, 0.05 M Na_2HPO_4 and 0.05 M KH_2PO, an electrolyte solution for electrochemical measurements (APB-KCl) consisting of 0.05 M CH_3COONa, 0.05 M Na_2HPO_4, 0.05 M KH_2PO_4 and 0.1 M KCl, and all other aqueous solutions were prepared by dissolving the respective reagents in ultra-high-quality water (UHQ) purified by a DEMIWA rosa 5 water purification system (WATEK, Czech Republic). A 40.0 mg/mL GOx solution was prepared in APB with pH 6.0. A 2.0 mg/mL AP solution was prepared in ethanol. Standard solutions of 0.1 M, 1.0 M and 2.0 M glucose, 1.0 M galactose, mannose, fructose, xylose and saccharose, and 0.1 M ascorbic acid and uric acid were prepared in APB-KCl (pH 5.5). To allow equilibration between the α- and β-anomeric forms, glucose and other saccharide solutions were prepared at least 24 h prior to experiments.

Synthesis of AuNPs

AuNPs were synthesised according to the standard method proposed by Turkevich et al. [14], based

on the reduction of $HAuCl_4$ by trisodium citrate in the presence of TA. 40.5 mL of a 0.01% aqueous solution of $HAuCl_4 \times 3\ H_2O$ was placed in an Erlenmeyer flask. Simultaneously, a second solution consisting of 8 mL of UHQ, 2 mL of 1% trisodium citrate and 12.5 µL of 1% TA was prepared in another Erlenmeyer flask. Both solutions, individually wrapped in aluminium foil, were heated to +60°C under continuous magnetic stirring. Upon reaching this temperature, the first solution was rapidly poured into the second solution under constant stirring. The resulting mixture was then heated to +98°C and maintained at this temperature for 3 min with continuous stirring. After completion of the reaction, the obtained red colloidal AuNPs solution was allowed to cool to room temperature and subsequently stored in a dark glass bottle at +4°C. The AuNPs synthesised using this method had an average diameter of approximately 13 nm and a concentration of 0.234 mM, as reported by German et al. [15].

Preparation of working electrodes

Graphite rods (150 mm in length, 3.0 mm in diameter and 99.999% purity) purchased from Sigma-Aldrich Chemie GmbH (Taufkirchen, Germany) were cut into segments approximately 4 cm in length. Prior to use, the rods were manually polished using successive grades of emery paper: fine (P120), very fine (P320) and ultra-fine (P2000). After polishing, the electrodes were thoroughly rinsed with ethanol and UHQ, dried at room temperature, and subsequently insulated with a silicone tube to prevent any contact between the lateral surface of the electrode and the electrolyte solution. Subsequently, a defined volume (0.0, 1.5, 3.0, or 6.0 µL) of a 2.0 mg/mL AP solution was drop-cast onto the GR electrode surface using a micropipette, and the solvent was allowed to evaporate at room temperature (GR/AP). Next, a defined volume (0.0, 1.5, 3.0, 6.0, 9.0, or 12.0 µL) of the AuNPs colloidal solution was drop-cast onto the GR/AP electrode surface and dried at room temperature (GR/AP/AuNPs). Finally, aliquots (3.0, 6.0, or 9.0 µL) of a 40.0 mg/mL GOx solution were deposited onto the GR/AP/AuNPs electrode surface and dried to obtain the GR/AP/AuNPs/GOx electrode. For enzyme cross-linking, the GR/AP/AuNPs/GOx electrode was placed in a closed test tube at a distance of 2 cm above a 25% GA solution and exposed to GA vapour at room temperature for 5.0, 10.0, 15.0, 20.0, or 25.0 min (GR/AP/AuNPs/GOx-GA). To remove non-cross-linked enzyme molecules, the modified electrode was thoroughly rinsed with UHQ. Prior to electrochemical measurements, the GR/AP/AuNPs/GOx-GA electrodes were stored in sealed test tubes above a drop of APB-KCl buffer (pH 5.5) at +4°C.

Electrochemical measurements

All electrochemical measurements were performed using a computer-controlled potentiostat/galvanostat Autolab PGSTAT 30 (Eco Chemie, Utrecht, The Netherlands) operated with the NOVA1.9 software. A conventional three-electrode electrochemical cell was employed, consisting of the GR/AP/AuNPs/GOx-GA electrode as the working electrode, a Pt counter electrode, and an $Ag/AgCl_{3.0\ M\ KCl}$ reference electrode. All experiments were carried out in 5.0 mL of the APB-KCl buffer with a fixed pH, inside a Faraday cage, at room temperature. Cyclic voltammograms were recorded over the potential range from –0.4 to +0.4 V at a scan rate of 0.05 V/s. Amperometric measurements were performed at a constant applied potential of +0.1 V, or at alternative potentials when required, while the electrolyte solution was continuously stirred at 400 rpm using a magnetic stirrer. The anodic current response of the biosensor to glucose was expressed as the change in current (ΔI), calculated as the difference between the current measured after the addition of a standard glucose solution and the background current recorded in APB-KCl. Unless otherwise stated, all experiments were performed in triplicate, and the results were presented as mean values with corresponding error bars representing the standard deviation.

RESULTS AND DISCUSSION

In this study, a reagentless amperometric glucose biosensor was fabricated by layer-by-layer adsorption of AP as a redox mediator, AuNPs and GOx onto a GR electrode, followed by chemical cross-linking of the adsorbed GOx molecules using GA vapour. The working electrode preparation procedure and the simplified operating principle of the biosensor are illustrated in Fig. 1. According to this operating principle, during glucose oxidation, electrons are transferred from glucose to GOx and subsequently accepted by the flavin adenine dinucleotide cofactor of GOx. The oxidised form

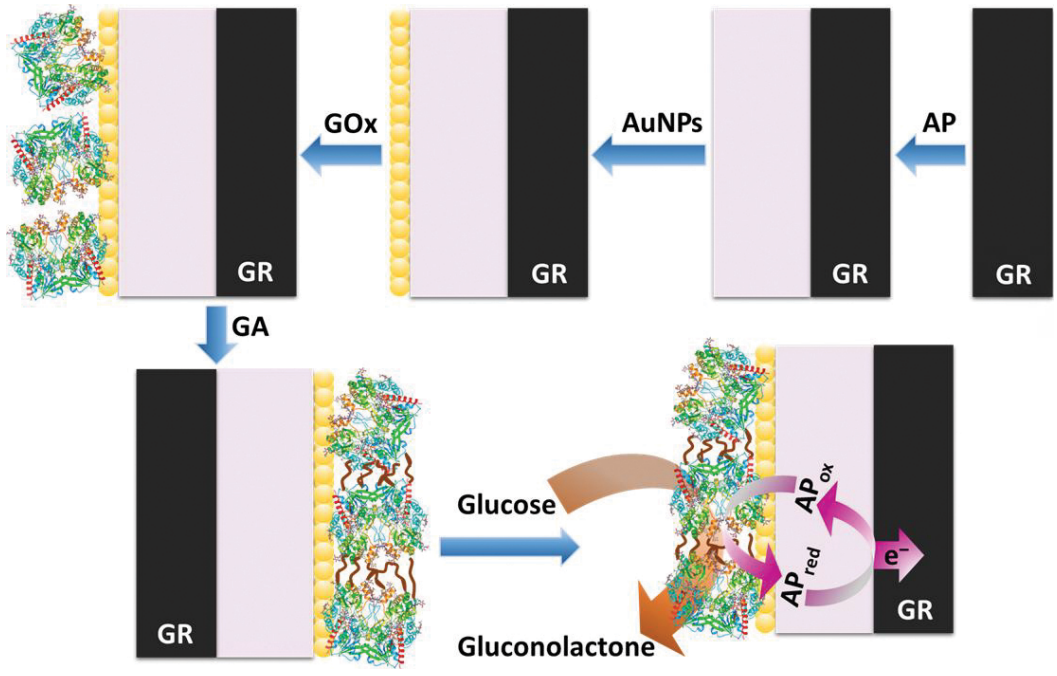

Fig. 1. The working electrode preparation procedure and the simplified operating principle of the developed biosensor

of the AP (AP_{ox}) then accepts electrons from the reduced GOx, being converted into its reduced form (AP_{red}), thereby regenerating the oxidised form of the enzyme. Finally, electrons are transferred from AP_{red} to the GR electrode surface, generating the anodic current proportional to the glucose concentration as AP is reoxidised. This biosensor design is advantageous due to non-diffusional, mediator-assisted electron transfer between the redox centre of GOx and the electrode surface, as well as the elimination of the need to add an external redox mediator to the sample solution prior to each measurement. Consequently, the proposed biosensor configuration is suitable for the development of clinical and self-monitoring devices, enabling routine and point-of-care glucose measurement [16, 17].

Optimisation of the working electrode modification conditions

The influence of the loading amounts of AP, GOx and AuNPs on the magnitude of the anodic current generated by the biosensor was investigated. The suitability of AP as a redox mediator was previously demonstrated by Oztekin et al. [18]. In that study, AP was identified as the most suitable mediator among the investigated 1,10-phenanthroline derivatives for glucose oxidase, enabling the development of reagentless GOx-based glucose biosensors. In view of those results, the influence of AP loading on the biosensor response was optimised in this study by varying the amount of AP while keeping the GOx loading constant. As shown in Fig. 2a, the anodic current response to glucose reached a maximum when 3.0 µL of 2.0 mg/mL (1.50 ± 0.08 µA) was deposited onto the GR/AP/GOx-GA electrode surface and decreased when a higher amount of AP was applied (0.60 ± 0.09 µA). This behaviour can be explained by the dual role of the adsorbed AP. At lower AP loadings, an increase in the amount of AP on the electrode surface enhances the biosensor response, as a larger number of mediator molecules are available to accept electrons from the reduced FAD cofactor of GOx and transfer them to the electrode, resulting in an increased anodic current. However, at higher AP loadings, the formation of a dense mediator layer on the electrode surface leads to a decrease in the effective electrical conductivity of the sensing interface and increases the electron transfer resistance [19], which in turn results in a reduced analytical signal generated by the GR/AP/GOx-GA-based biosensor.

Following the optimisation of AP loading, the effect of immobilised GOx amount on the biosensor response was evaluated by varying the GOx loading while keeping the AP amount constant. As shown in Fig. 2b, the anodic current response to glucose reached a maximum when 6.0 µL of

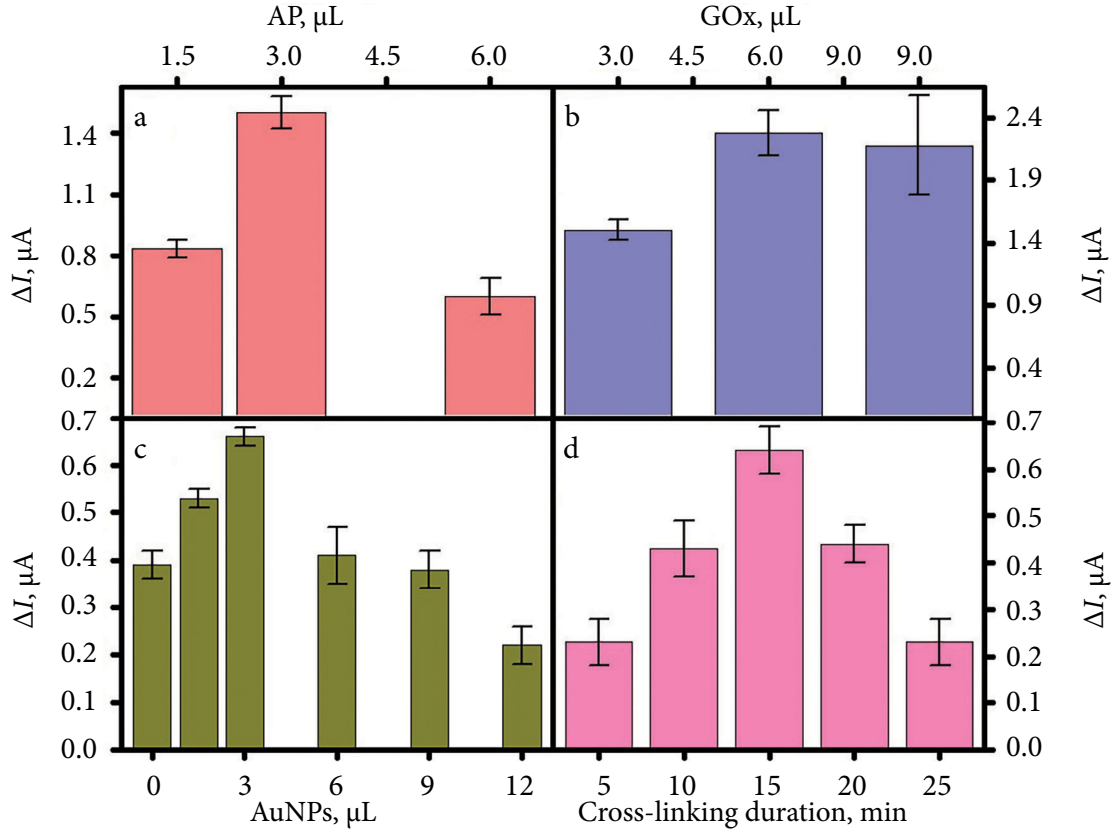

Fig. 2. Influence of the loading amounts of AP (a), GOx (b), and AuNPs (c) and the duration of GOx cross-linking with GA (d) on the magnitude of the anodic current response. Working electrode preparation conditions: (a) 3.0 µL of 40.0 mg/mL GOx, 15 min cross-linking duration; (b) 3.0 µL of 2.0 mg/mL AP, 15 min cross-linking duration; (c) 3.0 µL of 2.0 mg/mL AP, 6.0 µL of 40.0 mg/mL GOx, 15 min cross-linking duration; (d) 3.0 µL of 2.0 mg/mL AP, 3.0 µL of 0.234 mM AuNPs, 6.0 µL of 40.0 mg/mL GOx. Measurement conditions: APB-KCl (pH 6.0), applied potential of +0.1 V, 70.0 mM (a, b) or 10.0 mM (c, d) glucose

40.0 mg/mL was deposited onto the GR/AP/GOx-GA electrode surface (2.28 ± 0.18 µA), and decreased when a higher amount of GOx was applied (2.18 ± 0.40 µA). This behaviour can be explained by the fact that increasing the amount of GOx immobilised on the electrode surface initially enhances glucose oxidation due to an increased number of catalytically active sites. However, at higher GOx loadings, the formation of a thicker enzyme layer hinders glucose diffusion and limits the effective electron transfer between the enzyme, mediator and electrode. Similar effects have been observed in other studies reporting that thicker enzyme or immobilised films increase electron transfer resistance and slow substrate diffusion, resulting in the decreased amperometric response [20–23].

Subsequently, the influence of AuNPs loading on the biosensor response was examined while keeping the amounts of AP and GOx constant. As shown in Fig. 2c, the anodic current response to glucose reached a maximum when 3.0 µL of a 0.234 mM AuNPs colloidal solution was used to prepare the GR/AP/AuNPs/GOx-GA electrode (0.66 ± 0.02 µA), and decreased when higher amounts of AuNPs were applied. Such dependence of the analytical signal can be explained by the fact that AuNPs adsorbed on the electrode surface affect the efficiency of electron transfer and increase the electrode surface area, allowing for greater enzyme loading. AuNPs have been shown to enhance electron transfer and sensitivity in glucose biosensors by increasing the surface area and facilitating enzyme–electrode interactions. However, at higher AuNPs loadings, nanoparticle aggregation and changes in the effective surface structure can reduce electron transfer efficiency, leading to a decrease in the analytical signal [24, 25].

The influence of cross-linking of adsorbed GOx molecules using GA vapour on the magnitude of the anodic current generated by the biosensor was also investigated and is presented in Fig. 2d. The current response of the biosensor increased

with increasing the cross-linking duration and reached a maximum at a cross-linking time of 15 min (0.64 ± 0.05 μA), after which it decreased upon further prolongation of the cross-linking process. This behaviour can be explained by the degree of enzyme immobilisation and structural modification of the enzyme layer. At shorter cross-linking durations, GOx molecules are insufficiently cross-linked, resulting in a weaker attachment to the electrode surface and a partial enzyme desorption, which leads to a lower current response. Consequently, increasing the cross-linking duration improves enzyme retention on the electrode surface, resulting in an enhanced analytical signal. However, an excessive cross-linking at longer durations leads to the formation of a highly rigid and compact enzyme network, which increases diffusion resistance for glucose and limits electron transfer efficiency [26], thereby reducing the biosensor response. In addition, GA cross-links GOx molecules via free amino groups of lysine residues, which can cause an extensive enzyme modification, conformational changes, and a partial loss of catalytic activity [27, 28]. Therefore, the prolonged cross-linking ultimately led to a decrease in the analytical signal generated by the GR/AP/AuNPs/GOx-GA-based biosensor.

Considering the results of the GR/AP/AuNPs/GOx-GA electrode preparation optimisation and aiming to achieve the maximum biosensor sensitivity, the following conditions were selected for subsequent experiments: 3.0 μL of 2.0 mg/mL AP, 3.0 μL of 0.234 mM AuNPs, 6.0 μL of 40.0 mg/mL GOx, and a GOx cross-linking duration of 15 min.

Optimisation of biosensor operating conditions

After optimising the working electrode preparation conditions, the influence of the biosensor operating parameters on the current response was investigated, focusing on the applied potential and the pH of the electrolyte solution. The selection of the applied potential is a critical factor for amperometric biosensors, as increasing the potential enhances the driving force for electron transfer between the immobilised enzyme and the redox mediator, resulting in an increased amperometric response and improved biosensor sensitivity. However, operation at higher potentials may lead to a significant electrochemical interference from oxidisable species such as ascorbic acid and uric acid, which are commonly present in biological samples and can adversely affect the accuracy of glucose determination [29–31]. Therefore, the choice of the applied potential represents a compromise between sensitivity and selectivity. Based on these considerations, the effect of the applied potential on the biosensor current response was investigated by recording the amperometric signal in the potential range from −100 to +400 mV. As shown in Fig. 3a, the current response of the biosensor to glucose gradually increased with increasing the applied potential and reached a maximum at +100 mV, beyond which no further increase in current was observed. Taking into account the increased risk

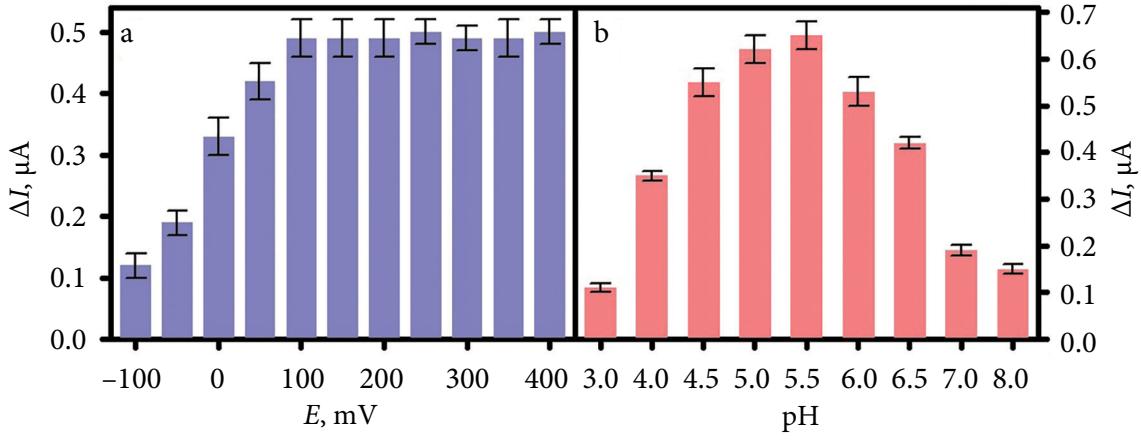

Fig. 3. The effect of the applied potential (a) and the pH of the APB-KCl electrolyte solution (b) on the current response of the biosensor. GR/AP/AuNPs/GOx-GA electrode preparation conditions: 3.0 μL of 2.0 mg/mL AP, 3.0 μL of 0.234 mM AuNPs, 6.0 μL of 40.0 mg/mL GOx, 15 min cross-linking duration. Measurement conditions: APB-KCl (pH 6.0 (a)), applied potential of +0.1 V (b), 10.0 mM glucose

of electrochemical interference at higher potentials and the reduced sensitivity at lower potentials, an applied potential of +100 mV was selected for all subsequent measurements.

Since pH of the electrolyte solution affects both the biocatalytic activity of the immobilised GOx and the electrochemical behaviour of redox mediator, the influence of pH on the magnitude of the anodic current generated by the biosensor was also investigated and is presented in Fig. 3b. The current response of the biosensor increased with increasing pH and reached a maximum at pH 5.5, after which it decreased upon further increase in pH. This behaviour is consisted with previously reported studies, which indicate that GOx exhibits a high catalytic activity in mildly acidic to near-neutral environments, typically within a pH range of 5.5–7.0, depending on the immobilisation conditions and local microenvironment of the enzyme [32–34]. Taking these results into account, an APB-KCl electrolyte solution with pH 5.5 was selected for all subsequent measurements.

Evaluation of the analytical performance of the biosensor

After the optimisation of the GR/AP/AuNPs/GOx-GA electrode preparation and operation conditions, the analytical performance of the developed biosensor was systematically evaluated, with key parameters including the linear detection range, LOD, LOQ, reproducibility, repeatability, storage stability, selectivity, and anti-interference capability. Figure 4a shows the relationship between glucose concentration and biosensor current response over a range of 0.30–100.0 mM, with a linear relationship (R^2 = 0.9999) observed for concentrations up to 10.0 mM (Fig. 4b). The LOD and LOQ, calculated as 3.3σ/slope and 10σ/slope, respectively, were determined to be 0.05 and 0.17 mM. These results demonstrate that the biosensor is suitable for practical applications, as glucose levels in human blood range from approximately 3 to 11 mM [35–37], while concentrations in food and beverage samples are typically higher; therefore, the biosensor provides the adequate sensitivity and dynamic range for the reliable glucose determination in both clinical and complex sample matrices.

Reproducibility and repeatability are key parameters for assessing biosensor performance, as they reflect the consistency and precision of the analytical signal under identical and varied experimental conditions [38, 39]. For the developed GR/AP/AuNPs/GOx-GA-based biosensor, repeatability was evaluated by calculating the relative standard deviation (RSD) of current responses to 10.0 mM glucose from three consecutive measurements using the same GR/AP/AuNPs/GOx-GA electrode (Fig. 5a), while reproducibility was determined

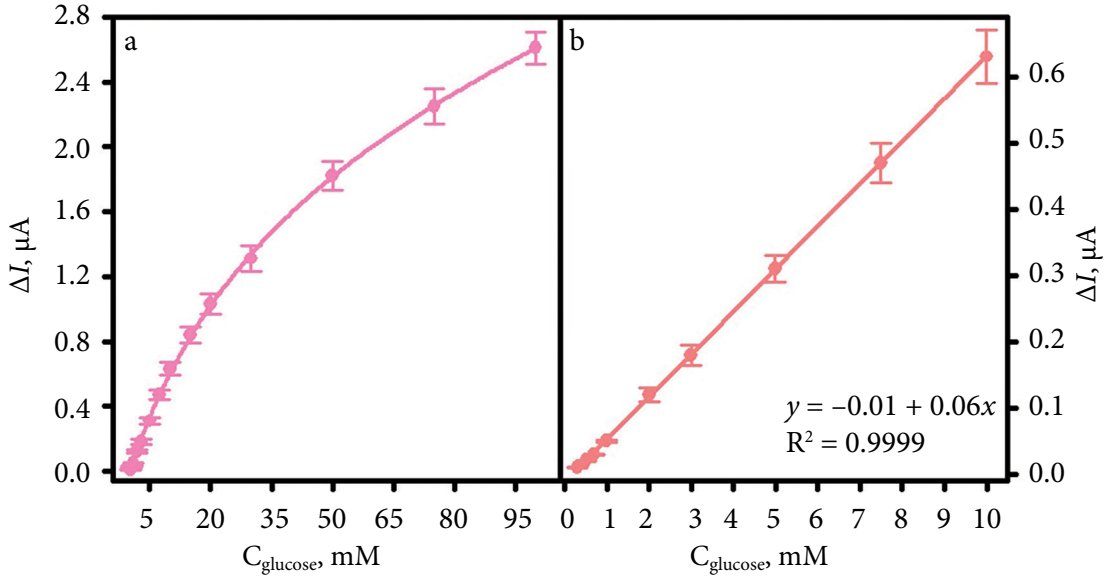

Fig. 4. Dependence of the biosensor current response on the glucose concentration (a) and calibration curve (b). GR/AP/AuNPs/GOx-GA electrode preparation conditions: 3.0 µL of 2.0 mg/mL AP, 3.0 µL of 0.234 mM AuNPs, 6.0 µL of 40.0 mg/mL GOx, 15 min cross-linking duration. Measurement conditions: APB-KCl (pH 5.5), applied potential of +0.1 V

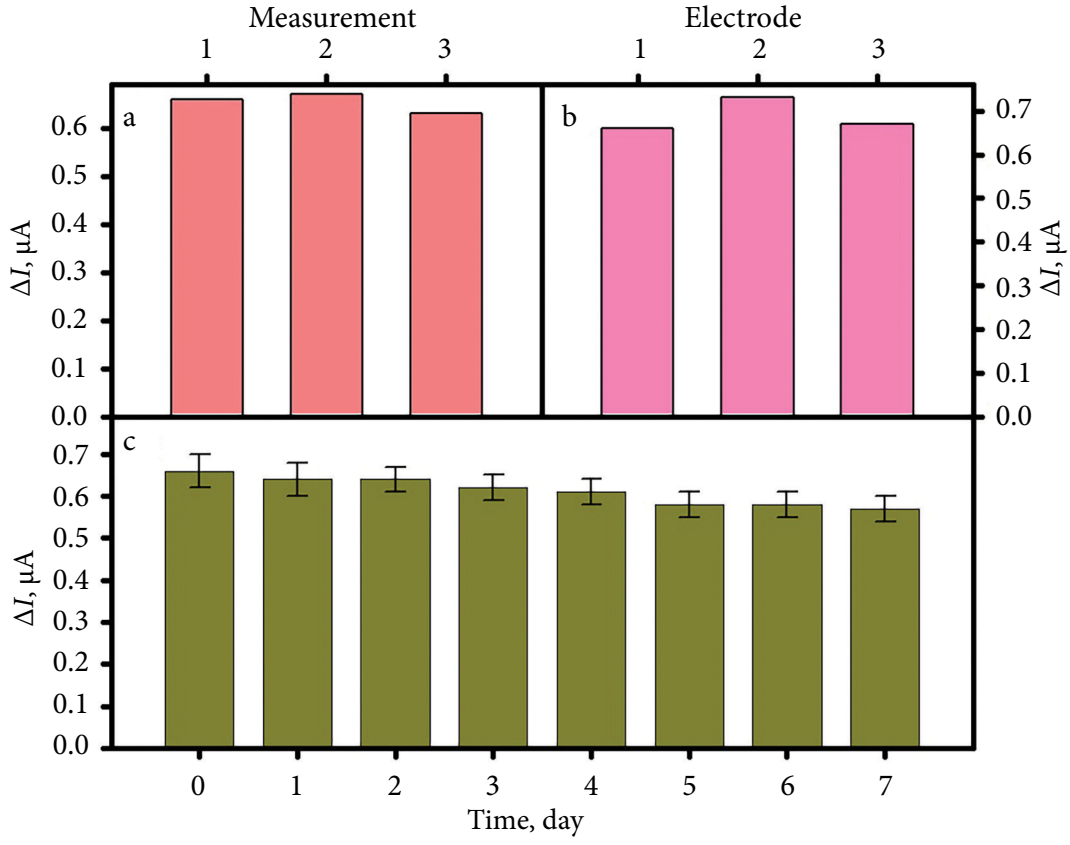

Fig. 5. Biosensor current responses to glucose recorded during repeatability (a), reproducibility (b), and storage stability (c) studies. GR/AP/AuNPs/GOx-GA electrode preparation conditions: 3.0 μL of 2.0 mg/mL AP, 3.0 μL of 0.234 mM AuNPs, 6.0 μL of 40.0 mg/mL GOx, 15 min cross-linking duration. Measurement conditions: APB-KCl (pH 5.5), applied potential of +0.1 V, 10.0 mM glucose

from three independently prepared electrodes under identical conditions (Fig. 5b). The calculated RSDs of 3.19 and 5.51%, respectively, demonstrate that the biosensor provides consistent responses both within a single electrode and across multiple electrodes. The slightly higher variation observed between different electrodes is likely due to minor differences in the surface loading and distribution of AP, AuNPs and GOx. These results confirm that the developed biosensor exhibits a reliable and reproducible performance, supporting its suitability for practical glucose measurements in both clinical and complex sample matrices.

The storage stability of the developed biosensor was evaluated by periodically measuring its amperometric response to 10.0 mM glucose over a 7-day period. Between measurements, the GR/AP/AuNPs/GOx-GA electrode was stored in a wet environment at +4°C. During the study period, the biosensor current response decreased from 0.66 ± 0.04 μA on the first day to 0.57 ± 0.03 μA on the seventh day, corresponding to approximately 86% retention of the initial current (Fig. 5c). Comparable glucose biosensor has demonstrated an approximately 77% signal retention after 16 days of storage at +4°C [22], and other design showed an approximately 96% retention after 7 days [40]. Therefore, the observed approximately 86% signal retention over 7 days indicates a competitive short-term storage stability and confirms the applicability of the biosensor for short- to mid-term practical use following calibration. While the gradual decrease in current response may be attributed to the partial dissociation of AP, AuNPs and GOx from the electrode surface and/or gradual inactivation of the GOx enzyme.

The selectivity of the developed biosensor was evaluated by recording its current response to different saccharides. First, a glucose standard solution was added to the electrochemical cell to obtain a concentration of 5.0 mM. After the current reached a stable value, standard solutions of galactose,

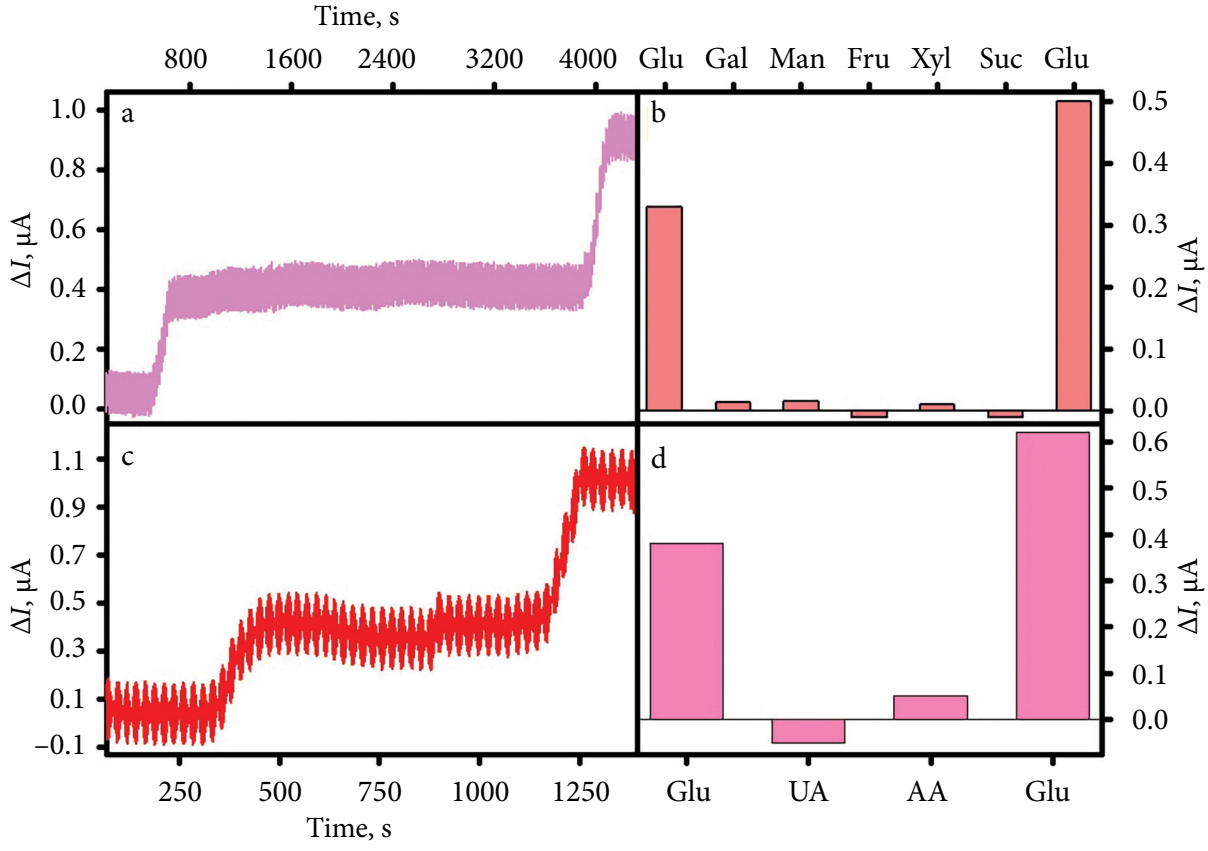

Fig. 6. Current response of the biosensor to glucose, other saccharides (a, b) and some interfering substances (c, d). GR/AP/AuNPs/GOx-GA electrode preparation conditions: 3.0 μL of 2.0 mg/mL AP, 3.0 μL of 0.234 mM AuNPs, 6.0 μL of 40.0 mg/mL GOx, 15 min cross-linking duration. Measurement conditions: APB-KCl (pH 5.5), applied potential of +0.1 V, 5.0 mM glucose (Glu), galactose (Gal), mannose (Man), fructose (Fru), xylose (Xyl) and sucrose (Suc), 10.0 mM glucose (a, b), 5.0 mM glucose, 0.3 mM uric acid (UA), 0.2 mM ascorbic acid (AA), 10.0 mM glucose (c, d)

mannose, fructose, xylose and sucrose (each at 5.0 mM) were sequentially introduced, followed by an additional addition of 10.0 mM glucose, and the corresponding current responses were recorded. As shown in Fig. 6a–b, none of the tested saccharides produced a significant change in the current response compared to glucose, indicating that the biosensor exhibits a high selectivity under the measurement conditions. This high selectivity can be attributed to the enzymatic specificity of GOx, which selectively catalyses the oxidation of glucose while exhibiting a negligible activity toward other saccharides [41, 42]. Therefore, the developed biosensor is well suited for the selective glucose determination in samples containing other saccharides.

One of the major challenges in amperometric glucose biosensors is interference from electroactive species that can be oxidised at the electrode surface during glucose determination in biological fluids. Among these, uric acid and ascorbic acid are considered the most significant interferents. In blood serum, uric acid concentrations typically range from 0.15 to 0.45 mM, while ascorbic acid concentrations vary between 0.04 and 0.14 mM [36]. These compounds undergo oxidation at the electrode surface, leading to an apparent increase in the measured current that is independent of glucose concentration. For this reason, the influence of uric acid and ascorbic acid on the current response of the developed biosensor was investigated. The measurements were performed by sequential addition of 5.0 mM glucose, 0.3 mM uric acid and 0.2 mM ascorbic acid, followed by an additional addition of 10.0 mM glucose. Both interferents caused approximately a 13% change in the biosensor current response (Fig. 6c–d). It should be noted, however, that the concentrations of the interfering substances employed in this study were relatively high, with the ascorbic acid

Table 1. **Comparison of the analytical characteristics of the developed biosensor and some previously published reagentless or AuNPs-enhanced amperometric glucose biosensors**

Working electrode	Applied potential, V	Linear range, mM	LOD, mM	LOQ, mM	Stability, %	Ref.
GR/AP/AuNPs/GOx-GA	+0.1	0.3–10.0	0.05	0.17	86 after 7 days	this work
GR/PD/AuNPs/GOx-GA	+0.3	0.1–10.0	0.024	–	–	[43]
GR/PD/GOx-GA	+0.2	0.1–76	0.025	–	23 after 16 days	[22]
GR/AuNPs/GOx-GA/Ppy	+0.3	0.99–19.9	0.2	–	31.6 after 21 days	[34]
GR/PPD/(AuNPs)PPCA-GOx	+0.2	0.2–150.0	0.08	–	3.98 after 14 days	[40]
GCE/Chi-Ppy/AuNPs/GOx	+0.4	1–20	0.068	–	67 after 50 days	[44]

PD, 1,10-phenanthroline-5,6-dione; Ppy, polypyrrole; PPD, poly(1,10-phenanthroline-5,6-dione); PPCA, poly(pyrrole-2-carboxylic acid); GCE, glassy carbon electrode; Chi, chitosan.

concentration exceeding typical levels found in real biological samples. Therefore, these results demonstrate that the developed biosensor exhibits an acceptable anti-interference capability toward these common electroactive species.

A comparison between the analytical performance of the developed biosensor and several previously reported reagentless or AuNPs-enhanced amperometric glucose biosensors is provided in Table 1. It demonstrates that in this work developed biosensor exhibits comparable or slightly improved analytical characteristics.

CONCLUSIONS

In this study, a reagentless amperometric glucose biosensor was successfully developed based on the layer-by-layer adsorption of AP, AuNPs and GOx onto a GR electrode, followed by chemical cross-linking of the adsorbed GOx molecules using GA vapour. AP acted as a redox mediator, enabling an efficient electron transfer from GOx to the electrode surface during enzymatically catalysed glucose oxidation, while AuNPs facilitated this electron transfer and enhanced the analytical signal. The biosensor design offers advantages such as non-diffusional, mediator-assisted electron transfer and the elimination of the need for an external redox mediator in the sample solution. The biosensor exhibited a wide linear range, low limits of detection and quantification, a high repeatability and an acceptable reproducibility, along with an excellent selectivity toward glucose, and a satisfactory storage stability and anti-interference capability towards uric and ascorbic acids. These features indicate that the biosensor is suitable for routine and point-of-care glucose measurements in clinical applications. Moreover, the proposed sensing platform can be readily adapted for the detection of other clinically or environmentally relevant analytes through an appropriate enzyme selection, highlighting its versatility and potential for broader analytical applications.

ACKNOWLEDGEMENTS

This research has received funding from the Research Council of Lithuania (LMTLT), Agreement No. S-MIP-24-7.

Received 19 February 2026
Accepted 25 February 2026

References

1. Y. Waly, A. Hussain, A. Al-Majmuei, et al., *Biosensors*, **16(1)**, 39 (2026).
2. X. Guo, J. Wang, J. Bu, et al., *ACS Omega*, **9(28)**, 30071 (2024).
3. F. B. Hu, *Diabetes Care*, **34(6)**, 1249 (2011).
4. Y. Zhi, S. Xie, B. Wei, *Clin. Chim. Acta*, **571**, 120221 (2025).
5. A. Kausaite-Minkstimiene, A. Krikstaponyte, N. Stasyuk, G. Gayda, A. Ramanaviciene, *Biosensors*, **15(8)**, 545 (2025).
6. J. A. Bauer, M. Zámocká, J. Majtán, V. Bauerová-Hlinková, *Biomolecules*, **12(3)**, 472 (2022).
7. C. M. Wong, K. H. Wong, X. D. Chen, *Appl. Microbiol. Biotechnol.*, **78**, 927 (2008).
8. J. Wang, *Chem. Rev.*, **108(2)**, 814 (2008).
9. L. Sakalauskiene, B. Brasiunas, A. Popov, A. Kausaite-Minkstimiene, A. Ramanaviciene, *Biosensors*, **13(10)**, 942 (2023).
10. N. German, A. Popov, A. Ramanaviciene, *Biosensors*, **14(3)**, 134 (2024).

11. K. Saha, S. S. Agasti, C. Kim, X. Li, V. M. Rotello, *Chem. Rev.*, **112(5)**, 2739 (2012).
12. G. Siciliano, A. Alsadig, M. S. Chiriacò, et al., *Talanta*, **268(1)**, 125280 (2024).
13. A. Karnwal, R. S. Kumar Sachan, I. Devgon, et al., *ACS Omega*, **9(28)**, 29966 (2024).
14. J. Turkevich, P. L. Stevenson, J. Hillier, *Discuss. Faraday Soc.*, **11**, 55 (1951).
15. N. German, A. Ramanavicius, J. Voronovic, A. Ramanaviciene, *Colloids Surf. A*, **413**, 224 (2012).
16. S. A. Pullano, M. Greco, M. G. Bianco, D. Foti, A. Brunetti, A. S. Fiorillo, *Theranostics*, **12(2)**, 493 (2022).
17. A. A. Karyakin, *Electrochem. Commun.*, **125**, 106973 (2021).
18. Y. Oztekin, V. Krikstolaityte, A. Ramanaviciene, Z. Yazicigil, A. Ramanavicius, *Biosens. Bioelectron.*, **26(1)**, 267 (2010).
19. R. Baronas, J. Kulys, *Sensors*, **8(8)**, 4800 (2008).
20. R. A. Croce Jr., S. Vaddiraju, F. Papadimitrakopoulos, F. C. Jain, *Sensors*, **12(10)**, 13402 (2012).
21. Q. Gao, Y. Guo, W. Zhang, H. Qi, C. Zhang, *Sens. Actuators B*, **153(1)**, 219 (2011).
22. A. Kausaite-Minkstimiene, R. Simanaityte, A. Ramanaviciene, L. Glumbokaite, A. Ramanavicius, *Talanta*, **171**, 204 (2017).
23. L. F. Ang, L. Y. Por, M. F. Yam, *PLoS One*, **10(3)**, e0111859 (2015).
24. W. Lipińska, K. Grochowska, K. Siuzdak, *Nanomaterials*, **11(5)**, 1156 (2021).
25. N. German, A. Ramanavicius, A. Ramanaviciene, *Sens. Actuators B*, **203**, 25 (2014).
26. L. Sakalauskiene, A. Popov, A. Kausaite-Minkstimiene, A. Ramanavicius, A. Ramanaviciene, *Biosensors*, **12(15)**, 320 (2022).
27. H. H. Nguyena, M. Kim, *Appl. Sci. Converg. Technol.*, **26(6)**, 157 (2017).
28. C. Mateo, J. M. Palomo, G. Fernandez-Lorente, J. M. Guisan, R. Fernandez-Lafuente, *Enzyme Microb. Technol.*, **40**, 1451 (2007).
29. C.-J. Yuan, C.-L. Hsu, S.-C. Wang, K.-S. Chang, *Electroanalysis*, **17**, 2239 (2005).
30. H. Deng, A. K. L. Teo, Z. Gao, *Sens. Actuators B*, **191**, 522 (2014).
31. K.-C. Lin, C.-Y. Yang, S.-M. Chen, D.-H. Zhao, Y.-S. Hou, *Int. J. Electrochem. Sci.*, **10(3)**, 2755 (2015).
32. M. Senel, C. Nergiz, *Synth. Met.*, **162**, 688 (2012).
33. S. P. Hendry, M. F. Cardosi, A. P. F. Turner, E. W. Neuse, *Anal. Chim. Acta*, **281**, 453 (1993).
34. N. German, A. Ramanavicius, A. Ramanaviciene, *Electroanalysis*, **29(5)**, 1267 (2017).
35. S. Zuliska, I. P. Maksum, Y. Einaga, G. T. M. Kadja, I. Irkham, *ADMET DMPK*, **12(3)**, 487 (2024).
36. A. Kausaite-Minkstimiene, L. Glumbokaite, A. Ramanaviciene, E. Dauksaite, A. Ramanavicius, *Electroanalysis*, **30**, 1642 (2018).
37. A. Kausaite-Minkstimiene, A. Kaminskas, G. Gayda, A. Ramanaviciene, *Biosensors*, **14(3)**, 138 (2024).
38. L.-C. Chen, E. Wang, C.-S. Tai, et al., *Biosens. Bioelectron.*, **155**, 112111 (2020).
39. C. I. L. Justino, A. C. Duarte, T. A. P. Rocha-Santos, *TrAC, Trends Anal. Chem.*, **85**, 36 (2016).
40. A. Kausaite-Minkstimiene, L. Glumbokaite, A. Ramanaviciene, A. Ramanavicius, *Microchem. J.*, **154**, 104665 (2020).
41. E. C. Adams, R. L. Mast, A. H. Free, *Arch. Biochem. Biophys.*, **91(2)**, 230 (1960).
42. J. F. Kornecki, D. Carballares, P. W. Tardioli, et al., *Catal. Sci. Technol.*, **10**, 5740 (2020).
43. N. German, A. Kausaite-Minkstimiene, A. Ramanavicius, T. Semashko, R. Mikhailova, A. Ramanaviciene, *Electrochim. Acta*, **169**, 326 (2015).
44. M. Senel, *Mater. Sci. Eng. C Mater. Biol. Appl.*, **48**, 287 (2015).

Katažyna Blaževič, Aistė Krikštaponytė, Anton Popov, Almira Ramanavičienė, Asta Kaušaitė-Minkštimienė

BEREAGENTIS AMPEROMETRINIS GLIUKOZĖS BIOLOGINIS JUTIKLIS 5-AMIN-1,10-FENANTROLINO, AUKSO NANODALELIŲ IR GLIUKOZĖS OKSIDAZĖS PAGRINDU

S a n t r a u k a

Gliukozės koncentracijos stebėsena yra būtina siekiant suvaldyti cukrinį diabetą ir užtikrinti tikslią analizę klinikiniuose bei maisto tyrimuose. Šiame darbe, ant grafito strypo elektrodo paviršiaus sluoksnis po sluoksnio adsorbuojant 5-amin-1,10-fenantroliną (AP), 13 nm skersmens aukso nanodaleles (AuNPs) ir gliukozės oksidazę (GOx), o vėliau GOx molekules chemiškai sujungiant skersiniais ryšiais glutaro aldehido garais, buvo sukurtas bereagentis amperometrinis gliukozės biologinis jutiklis. Tokioje konstrukcijoje AP veikė kaip redokso mediatorius, užtikrinantis efektyvią elektronų pernašą, o AuNPs stiprino analizinį signalą. Sukurtas biologinis jutiklis pasižymėjo plačiu tiesiniu diapazonu (0,30–10,0 mM), žemomis aptikimo ir nustatymo ribomis, atitinkamai 0,05 ir 0,17 mM, dideliu pakartojamumu (santykinis standartinis nuokrypis (SSN) 3,19 %) ir priimtinu atkuriamumu (SSN 5,51 %), taip pat puikiu atrankumu gliukozei bei patenkinamu saugojimo stabilumu (86 % signalo išlaikymas per 7 dienas) bei atsparumu urino ir askorbo rūgščių interferencijai. Šios savybės rodo, kad sukurtas biologinis jutiklis yra tinkamas rutininiam ir sveikatos priežiūros įstaigose atliekamam gliukozės koncentracijos nustatymui. Be to, biologinio jutiklio konstrukcija pasižymi universalumu ir gali būti pritaikoma kitų kliniškai ar aplinkos požiūriu svarbių analičių nustatymui, atskleidžiant platesnio analitinio taikymo potencialą.